IEICE TRANS. ELECTRON., VOL.E107–C, NO.5 MAY 2024

BRIEF PAPER

Optical Mode Multiplexer Using $LiNbO_3$ Asymmetric Directional Coupler Enabling Voltage Control for Phase-Matching Condition

Shotaro YASUMORI[†], ***Student Member***, **Seiya MORIKAWA**[†], ***Nonmember***, **Takanori SATO**[††], ***Member***, **Tadashi KAWAI**[†], ***Senior Member***, **Akira ENOKIHARA**[†a)], ***Member***, **Shinya NAKAJIMA**[†††], ***Nonmember***, ***and*** **Kouichi AKAHANE**[†††], ***Member***

SUMMARY An optical mode multiplexer was newly designed and fabricated using $LiNbO_3$ waveguides. The multiplexer consists of an asymmetric directional coupler capable of achieving the phase-matching condition by the voltage adjustment. The mode conversion efficiency between TM_0 and TM_1 modes was quantitatively measured to be 0.86 at maximum.

key words: *optical mode multiplexer, asymmetric directional coupler, $LiNbO_3$ waveguide, phase-matching condition*

1. Introduction

Optical communication systems based on mode-division multiplexing using multimode optical fibers are expected to support future high-capacity information transmission [1], [2]. One of the important devices to excite and control the multiple propagation modes separately is a mode multiplexer/demultiplexer, and its fundamental function is mode conversion. Asymmetric directional couplers (ADCs) [3]–[5] and multimode interference structures [6], [7] have been used for mode conversion. These are with optical waveguide structures and have advantages in operational stability and integration with other waveguide elements. Among them, ADCs have a simple structure and high scalability, and Si-based waveguide materials were mainly used for them in previous studies [3], [5], [8]. However, since severe phase-matching conditions are necessary for the ADCs to achieve high mode conversion efficiency, high accuracy in the design process and a stable operating environment may be required for Si-based ADC devices.

On the other hand, the electro-optic material $LiNbO_3$ (LN) is widely used as a substrate for high-speed optical modulators [9], and low-loss optical waveguides are easily obtained by Ti thermal diffusion. Therefore, if ADC devices are designed using Ti-diffused LN (Ti:LN) waveguides, they can be integrated with electro-optic devices such as optical modulators. Moreover, the device characteristics can be voltage-controlled using the electro-optic effect, which is expected to improve the device characteristics and relax the fabrication accuracy. In particular, it is highly advantageous to achieve the phase-matching condition by the voltage control after device fabrication. Previous studies on ADCs using LN waveguides have been reported analyzing the characteristics of polarization splitters [10] and tunable wavelength filters [11]. An ADC with LN ridge waveguides was also presented to apply to a mode converter capable of wavelength switching [12]. However, there have yet to be reported LN waveguide ADCs where the mode conversion efficiency was improved by voltage control due to the electro-optic effect, as far as the authors know.

In this paper, we report on the design and fabrication of ADCs using Ti:LN optical waveguides, and the experimental demonstration that the phase-matching condition between TM_0 and TM_1 modes was achieved by adjusting the voltage to maximize the mode conversion efficiency.

2. Design of Asymmetric Directional Coupler for Mode Conversion

The basic structure of a waveguide type ADC is shown in Fig. 1. Two optical waveguides of different widths, the wider one called the bus waveguide and the narrower one called the access waveguide, are placed parallel and close together in the coupling section. Assuming TM mode propagation, the TM_{0A} mode, which is the fundamental mode, TM_0 mode, of the access waveguide (width W_A), is coupled with the TM_{1B} mode, which is the next higher-order mode, TM_1 mode, of the bus waveguide (width W_B). Here, it is essential to realize the phase-matching condition for efficient mode conversion. That is, the effective refractive indices n_{0A} and n_{1B} of the TM_{0A} and TM_{1B} modes, respectively, are matched ($n_{0A} = n_{1B}$) and the propagation velocities of both modes are identical. At the coupling section, the TM_{0A} and TM_{1B} modes couple to produce two supermodes. Let $\Delta\beta$ be the difference in phase constants between the two supermodes, length L of the coupling section for complete mode conver-

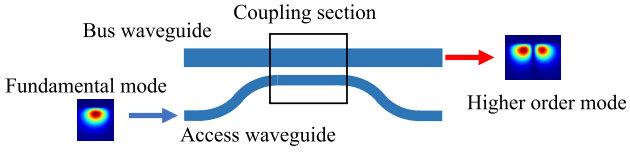

Fig. 1 Basic structure of a waveguide-type asymmetric directional coupler.

Manuscript received September 7, 2023.
Manuscript revised October 24, 2023.
Manuscript publicized November 29, 2023.

[†]The authors are with Graduate School of Engineering, University of Hyogo, Himeji-shi, 671–2280 Japan.
[††]The author is with Graduate School of Information Science and Technology, Hokkaido University, Sapporo-shi, 060–0814 Japan.
[†††]The authors are with National Institute of Information and Communications Technology, Koganei-shi, 184–8795 Japan.
a) E-mail: enokihara@eng.u-hyogo.ac.jp

DOI: 10.1587/transele.2023ECS6011

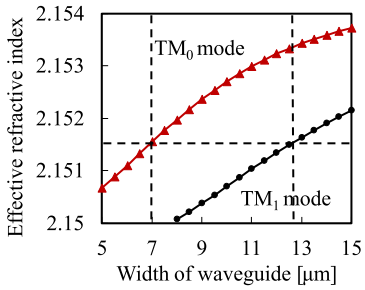

Fig. 2 Effective refractive indices of the TM_0 and TM_1 modes as a function of width of Ti:LN optical waveguides at 1.55 μm wavelength.

sion is $L = \pi/\Delta\beta$ at the minimum, where all the energy of the TM_{0A} mode is transferred to the TM_{1B} mode. This L is denoted as the coupling length L_c.

Next, the refractive index distribution of the Ti:LN optical waveguide was calculated [13], [14], and then the scalar finite element method (SFEM) [15] was used to analyze the guided modes (for simplicity, anisotropy of LN was not considered here). Figure 2 shows the effective refractive indices of the TM_0 and TM_1 modes as a function of the optical waveguide width at a 1.55 μm light wavelength. Our standard waveguide fabrication conditions for a z-cut LN substrate are used for the calculation: Ti-film thickness of 85 nm, diffusion temperature of 1070°C, and diffusion time of 7.8 hours. It is seen that at 7 μm width, the single-mode propagation condition is satisfied, and the effective refractive index of the TM_0 mode is almost the same as that of the TM_1 mode at around 13 μm width. Therefore, we used ADCs with the access waveguide width fixed at $W_A = 7$ μm and the bus waveguide width W_B at around 13 μm in our experiments.

3. Voltage Control for Phase-Matching Condition

As shown in Fig. 3, electrodes made of metal films are formed on the optical waveguides of the coupling section. When a voltage V_c is applied between the electrodes, an electric field is generated in both waveguides in opposite directions, and the refractive indices of the access waveguide and bus waveguide change in opposite directions due to electro-optic effects in the z-cut LN substrate. Thereby the difference between n_{0A} and n_{1B} can be eliminated by adjusting the voltage to achieve the phase-matching condition. The electric field distribution induced by the applied voltage V_c was obtained analytically using the conformal mapping method [16], and then we calculated n_{0A} and n_{1B} by the SFEM taking account of the field distribution. Figure 4 shows n_{0A} and n_{1B} versus V_c for $W_A = 7$ μm, $W_B = 13$ μm, and the waveguide spacing $G = 6$ μm. It is seen that the difference between n_{0A} and n_{1B} can be eliminated by the adjustment of V_c, resulting in satisfying the phase-matching condition.

4. Fabrication and Evaluation

Several ADCs of $W_A = 7$ μm, $G = 6$ μm, $W_B = 12$~14 μm,

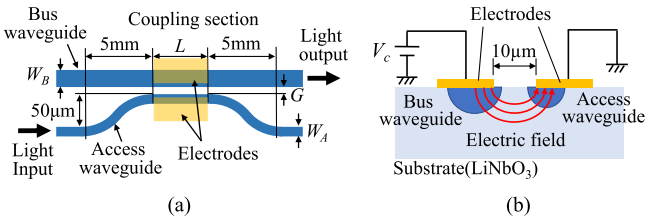

Fig. 3 Structure of ADC with electrodes for voltage control, (a) top view and (b) cross sectinal view at the coupling section.

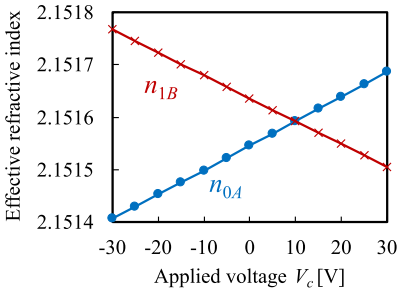

Fig. 4 Effective refractive indices n_{0A} and n_{1B} versus the applied voltage V_c calculated for $W_A = 7$ μm, $W_B = 13$ μm, and $G = 6$ μm.

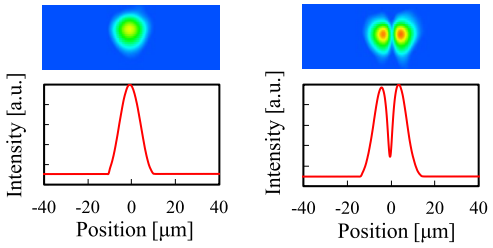

Fig. 5 Electric field intensity distribution of the output light at the edge surface of the substrate, (a) for the access waveguide and (b) for the bus waveguide.

and $L = 1$~5 mm were fabricated and evaluated. The optical waveguides were formed on a 0.5-mm-thick z-cut LN substrate by thermal diffusion of an 85-nm-thick Ti film at 1070 °C for 7.8 hours. A 0.5 μm-thick gold film was patterned for the electrodes by the lift-off process. The electric field profiles of the propagating lightwaves of the access and the bus waveguide were observed. Figure 5 shows the electric field intensity distribution of the output light at the edge surface of the substrate measured by an infrared camera where TM waves of 1.55 μm wavelength were input to the access waveguide. Since only the TM_1 mode was output from the bus waveguide, TM_{0A} - TM_{1B} mode conversion was confirmed.

Figures 6 show the output light intensity I_B from the bus waveguide when a lightwave was input to the access waveguide, where I_B on the vertical axis is normalized to the maximum value. The change of I_B with L at $W_B = 13$ μm is presented in Fig. 6 (a), where the maximum is observed at $L = 5$ mm. Figure 6 (b) shows I_B in the range of $W_B = 12$ to 14 μm at $L = 5$ mm. I_B is maximum around $W_B = 13$ μm. The phase-matching condition was expected to be satisfied around $W_B = 13$ μm, which agrees with the analytical results

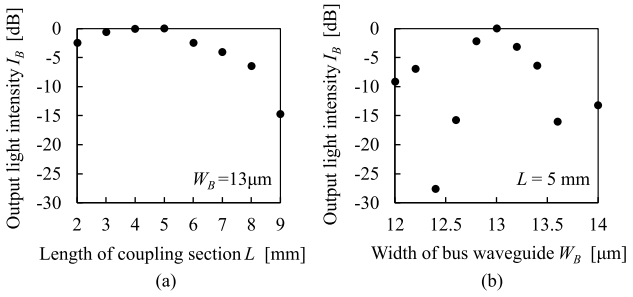

Fig. 6 Output light intensity I_B from the bus waveguide when a lightwave is input to the access waveguide measured (a) as a function of L and (b) as a function of W_B, where I_B is normalized to the maximum value.

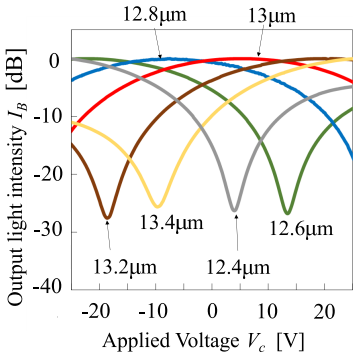

Fig. 7 Output light intensity I_B from the bus waveguide measured as a function of the applied voltage V_c, where the values in the figure represent W_B.

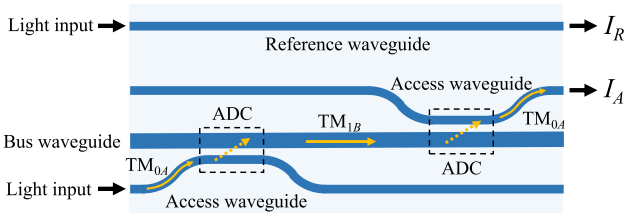

Fig. 8 Test device consisting of two ADCs of the same structure for the quantitative measurement of the optical power conversion efficiency T_{10} from the TM_{0A} mode to the TM_{1B} mode.

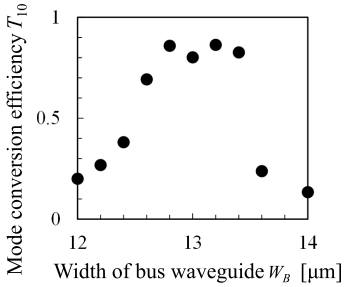

Fig. 9 Mode conversion efficiency T_{10} maximized by adjusting the voltage V_C measured for ADCs with W_B = 12 to 14μm using the test device in Fig. 8.

in Fig. 2.

The measurement results of I_B as a function of V_c with W_B = 13 μm and L = 5 mm are shown in Fig. 7, where I_B is normalized to a maximum value for each W_B. It is seen that I_B changes with V_c and maximizes at different values of V_c for each W_B. This is because the effective refractive index difference ($n_{0A} - n_{1B}$) between the TM_{0A} and TM_{1B} modes changed with V_c and the phase-matching condition was achieved at those values of V_c. And I_B could be maximized for W_B in the range of 12.4 to 13.6 μm by the voltage of V_c = −25 to +25 V.

We quantitatively evaluated the mode conversion efficiency T_{10}, which means the optical power transmission from the TM_{0A} mode to the TM_{1B} mode. Using the usual measurement method by end-face coupling of a single-mode optical fiber, it is difficult to accurately measure the optical power of higher modes, such as the TM_1 mode. Therefore, as shown in Fig. 8, we fabricated an evaluation test device consisting of two ADCs of the same structure connected in series. The input light to the access waveguide is converted to the TM_{1B} mode of the bus waveguide in the front ADC and then converted back to the TM_{0A} mode of the access waveguide again in the rear ADC. A reference waveguide of the same width as the access waveguide was formed on the same substrate surface. Denoting I_R and I_A as the optical output power from the reference and access waveguides, respectively, when the same optical power is input to the reference and access waveguides, the mode conversion efficiency T_{10} of the single ADC can be expressed by $\sqrt{I_A/I_R}$. In this measurement for T_{10}, since the input and output of lightwaves are performed by the end face coupling with single-mode waveguides of 7 μm width, the waveguide loss is also canceled out.

Figure 9 shows the measurement results of T_{10} which was maximized by adjusting the voltage V_c, where the test device with ADCs for W_B = 12 to 14 μm was used. Excellent values of T_{10} of more than 0.8, which are corresponding mode conversion losses of less than 1 dB, were achieved in the range of W_B = 12.8 to 13.4 μm. The phase-matching condition was realized by the voltage adjustment, and a maximum T_{10} of 0.86 (conversion loss of 0.66 dB) was obtained at W_B = 13.2 μm. These results demonstrate that the proposed ADC can achieve the phase-matching condition by the voltage adjustment.

5. Conclusion

An optical waveguide mode multiplexer for TM_0 and TM_1 modes using ADCs with LN waveguides was proposed, and a maximum mode conversion efficiency of 0.86 was obtained. The phase-matching condition was achieved by the voltage adjustment. This function effectively relaxes the precision in device design and fabrication and compensates for deviations of device properties induced by changes in the operating environment. Furthermore, the mode multiplexer can be integrated with other EO devices, such as an optical modulator, to expect to realize highly functional mode control devices.

Acknowledgments

We thank Professor Tetsuya Kawanishi of Waseda University and Professor Atsushi Kanno of Nagoya Institute of Technology for their valuable cooperation in this research, and Mr. Sohei Miyamoto of Mitsubishi Electric Corporation for his assistance in the experiments. This work was partially supported by the Hyogo Science and Technology Association and by JSPS KAKENHI Grant number 20K04601.

References

[1] P. Sillard, M. Bigot-Astruc, and D. Molin, "Few-mode fibers for mode-division-multiplexed systems," J. Lightw. Technol, vol.32, no.16, pp.2824–2829, Aug. 2014.

[2] G. Rademacher, R.S. Luís, B.J. Puttnam, T.A. Eriksson, E. Agrell, R. Maruyama, K. Aikawa, H. Furukawa, Y. Awaji, and N. Wada, "159 Tbit/s C+L band transmission over 1045 km 3-mode graded-index few-mode fiber," 2018 Optical Fiber Communications Conference (OFC), Th4C.4, 2018.

[3] J. Wang, P. Chen, S. Chen, Y. Shi, and D. Dai, "Improved 8-channel silicon mode demultiplexer with grating polarizers," Opt. Express, vol.22, no.11, pp.12799–12807, June 2014.

[4] T. Sato, T, Fujisawa, and K. Saitoh, "Ultra-robust design of mode (de)multiplexer based on asymmetrical directional coupler using wire and one-side rib waveguides," 2019 24th OptoElectronics and Communications Conference (OECC) and 2019 International Conference on Photonics in Switching and Computing (PSC), TuE2-3, July 2019.

[5] J. Takano, T. Sato, Y. Sawada, T. Fujisawa, T. Sakamoto, T. Matsui, K. Tsujikawa, K. Nakajima, and K. Saitoh, "Proposal of Si four-wavelength multiplexer using higher-order mode for 100GbE," Proc. 23rd OptoElectronics and Communications Conference (OECC 2018), 4E2-4, July 2018.

[6] Y. Kawaguchi and K. Tsutsumi, "Mode multiplexing and demultiplexing devices using multimode interference couplers," Electron. Lett., vol.38, no.25, pp.1701–1702, Dec. 2002.

[7] J. Leuthold, J. Eckner, E. Gamper, P.A. Besse, and H. Melchior, "Multimode interference couplers for the conversion and combining of zero- and first-order modes," J. Lightw. Technol, vol.16, no.7, pp.1228–1239, July 1998.

[8] C. Ye and D. Dai, "Ultra-Compact Broadband 2×2 3 dB Power Splitter Using a Subwavelength-Grating-Assisted Asymmetric Directional Coupler," J. Lightw. Technol., vol.38, no.8, pp.2370–2375, April 2020.

[9] Y. Yamaguchi, A. Kanno, T. Kawanishi, M. Izutsu, and H. Nakajima, "Precise Optical Modulation Using Extinction-Ratio and Chirp Tunable Single-Drive Mach–Zehnder Modulator," J. Lightw. Technol, vol.35, no.21, pp.4781–4788, Nov. 2017.

[10] H. Luo, Z. Chen, H. Li, L. Chen, Y. Han, Z Lin, S. Yu, and X. Cai, "High-performance polarization splitter-rotator based on Lithium Niobate-on-insulator platform," J. Lightw. Technol, vol.33, no.24, pp.1423–1426, Dec. 2021.

[11] R. Chakraborty, "Design of tunable asymmetric directional coupler filter using periodically segmented Ti:$LiNbO_3$ waveguides," Optik vol.125, no.19, pp.5816–5819, Oct. 2014.

[12] M. Zhang, W. Ai, K. Chen, W. Jin, and K.S. Chiang, "A Lithium-Niobate waveguide directional coupler for switchable mode multiplexing," IEEE Photon. Technol. Lett., vol.30, no.20, pp.1764–1767, Sept. 2018.

[13] M. Fukuma and J. Noda, "Optical properties of titanium-diffused $LiNbO_3$ strip waveguides and their coupling-to-a-fiber characteristics," Appl. Opt., vol.19, no.4, pp.591–597, Feb. 1980.

[14] S. Fouchet, A. Carenco, C. Daguet, R. Guglielmi, and L. Riviere, "Wavelength dispersion of Ti induced refractive index change in $LiNbO_3$ as a function of diffusion parameters," J. Lightw. Technol., vol.5, no.5, pp.700–708, May 1987.

[15] M. Koshiba, Optical Waveguide Theory by the Finite Element Method, Springer, Dordrecht, 1993.

[16] O.G. Ramer, "Integrated optic electrooptic modulator electrode analysis," IEEE J. Quantum Electron., vol.QE-18, no.3, pp.386–392, March 1982.